


# A rare case of atypical skull base meningioma with perineural spread

Henry Walton<sup>1\*</sup>, Simon Morley<sup>1</sup>, Javier Alegre-Abarrategui<sup>2</sup>

1. Department of Radiology, University College Hospital, London, UK

2. Department of Neuropathology, National Hospital for Neurology and Neurosurgery, London, UK

\* **Correspondence:** Henry Walton, Imaging Department, Podium Level 2, University College Hospital, 235 Euston Road, London NW1 2BU, UK

 [henry.walton@nhs.net](mailto:henry.walton@nhs.net)

Radiology Case. 2015 Dec; 9(12):1-14 :: DOI: 10.3941/jrcr.v9i12.2648

## ABSTRACT

Atypical meningioma is a rare cause of perineural tumour spread. In this report, we present the case of a 46-year-old female with an atypical meningioma of the skull base demonstrating perineural tumour spread. We describe the imaging features of this condition and its distinguishing features from other tumours exhibiting perineural spread.

## CASE REPORT

### CASE REPORT

#### Presentation

A 46-year-old female presented with three months of left sided facial numbness, jaw pain and headache on a background of progressive ipsilateral hearing loss over two years. There was no past medical, social or family history of note. On examination, there was sensory loss in the distribution of the maxillary and mandibular branches of the left trigeminal nerve, complete left sided deafness and a decreased left corneal reflex.

#### Imaging

Magnetic resonance imaging (MRI) revealed a large left sided skull base mass. The mass extended above and below the skull base by perineural spread through the foramen ovale and foramen rotundum. The mass measured 4.8 x 4.8 x 6.4cm in maximal dimensions. The mass was isointense to muscle on T1 weighted (T1) imaging (Fig. 1a-c) and hyperintense on T2 weighted (T2) imaging (Fig. 2). Post-contrast, the tumour displayed intense, homogeneous enhancement (Fig. 1d-f). On diffusion-weighted imaging (DWI), there was restricted diffusion and low apparent diffusion coefficient (ADC) value throughout the tumour (Fig. 3). Inferiorly, the tumour involved the nasopharynx resulting in obstruction of the left Eustachian tube (Fig. 4). Intracranially, the tumour was extra-axial, extending along the surface of the greater wing of the left

sphenoid via an enhancing dural tail (Fig. 1d,e). Posteriorly, the mass bulged through Meckel's cave into the prepontine cistern where it was inseparable from the trigeminal nerve (Fig. 5). Anteriorly, the mass extended into the pterygopalatine fossa and through the wall of the sphenoid sinus and sphenopalatine foramen into the nasal cavity (Fig. 6,7). There was denervation atrophy of the left pterygoid, temporalis and masseter muscles (Fig. 8).

Computed tomography (CT) of the head and neck revealed internal calcification within the intracranial component of the mass (Fig 9). There was widening and erosion of the foramen rotundum and foramen ovale (Fig. 11). There was hyperostosis of the surrounding sphenoid bone and bony erosion of nasal septum, the posterior maxillary alveolar margin and the left lateral wall of the sphenoid sinus (Fig. 8,10,12).

#### Histology

Tissue samples were initially obtained by a percutaneous CT guided core biopsy. The samples were fragmented and difficult to assess histologically. Two pathologists reviewed the samples independently arriving at differing histological diagnoses. One pathologist diagnosed a plasmacytoid neoplasm and the other diagnosed a benign meningioma. Given this discrepancy, a second percutaneous CT-guided core biopsy was performed. This sample exhibited differentiated

meningothelial cells with an increased mitotic rate and prominent nucleoli (Fig.13a). Throughout the sample there were areas of patternless sheet-like growth and small foci of necrosis (Fig13b). Based upon these features, a definitive diagnosis of atypical meningioma was made.

#### *Management*

The tumour was deemed too extensive for complete resection. The surgical team performed a two-step partial tumour resection - a maxillotomy to debulk the extracranial portion of tumour and a posterior fossa craniotomy to excise of the cerebellopontine angle tumour. Two months after surgery, the patient commenced a six-week course of adjuvant intensity-modulated radiotherapy with 54 Gray delivered in 30 daily fractions.

#### *Follow-up*

At the last clinical review, the patient was four months post radiotherapy and had benefitted from alleviation of her headache and facial pain. All other clinical features were stable. Follow-up MRI scans have shown a stable appearance of the residual tumour (Fig.14).

## DISCUSSION

Meningiomas are meningeothelial cell neoplasms, classically attached to the inner surface of the dura mater. They are subclassified as benign, atypical and malignant corresponding to World Health Organisation (WHO) grades I, II, and III respectively(1). Meningiomas possess mixed features of epithelial and mesenchymal cells. Atypical meningiomas are distinguished from benign meningiomas by increased mitotic activity, prominent nucleoli, uninterrupted patternless growth and foci of spontaneous necrosis. Malignant meningiomas have a greatly increased mitotic rate and features of frank anaplasia(1). Perineural spread is a mechanism whereby tumour spreads along the loose connective tissues of the perineurium.

#### *Epidemiology:*

Meningiomas are the most common non-glial tumours of the central nervous system. With an annual incidence of 6 per 100,000, they account for 16-20% of all intracranial tumours(2-4). Atypical meningiomas represent 4.7-7.2% of all meningiomas(5). Benign meningiomas are more common in those aged over 60 years and in females (M:F 1:2.3) whereas atypical meningiomas occur 10 years earlier on average and are more common in men (M:F 1:0.9)(6). Though perineural tumour spread is a common phenomenon in several head and neck malignancies, it has rarely been reported in meningiomas, with only 3 published cases to date(7-9).

#### *Etiology:*

Benign meningiomas arise following a genetic mutation on chromosome 22q12(4,10). This genetic locus encodes for the tumour suppressor protein schwannomin (also known as merlin), the same protein that is involved in neurofibromatosis type 2 (NF2). Loss of Schwannomin has a variety of biological effects that lead to a higher risk of developing benign meningiomas. Accumulation of further chromosomal

mutations is thought to cause the transformation to atypical and malignant meningiomas. This transformation can occur de novo in existing benign meningioma or during tumour recurrence(4,10). Exposure to ionising radiation is the only widely recognised environmental risk factor for meningiomas(4,10,11).

#### *Clinical Findings:*

Common clinical findings in skull base meningiomas include impaired vision, hearing and smell as well as headache, exophthalmos and seizures depending on the position of the tumour(11-14). Perineural spread commonly affects the maxillary and mandibular branches of the trigeminal nerve(15,16). It is important to recognise that even when there is extensive perineural spread, a large proportion of patients (30-45%) remain asymptomatic with a normal cranial nerve examination(16-18). When clinical features are present, they include pain and sensory loss in a maxillary and mandibular distribution and subtle unilateral weakness of the muscles of mastication. Due to vague and non-specific features, affected patients are commonly misdiagnosed with Bell's palsy or trigeminal neuralgia at initial presentation(19,20).

#### *Imaging findings:*

##### *Meningioma*

Meningiomas typically appear as homogeneous, hemispheric, lobular, broad-based, extra-axial masses with well-circumscribed margins and a homogeneous, avid enhancement pattern on cross-sectional imaging(11,21). The most reliable imaging feature is a "dural tail," the presence of which infers a diagnostic sensitivity of 58% and a specificity of 94%(11). On CT, meningiomas are homogeneously hyperattenuating (72%) and cause peritumoral vasogenic oedema in the adjacent brain parenchyma (52%). They frequently display areas of internal calcification (27%) and cause hyperostosis of the adjacent bone (18%)(21). On MRI, meningiomas are iso- to hypointense on T1 sequences and iso- to hyperintense on T2. A cerebrospinal fluid (CSF) cleft is a commonly encountered (80%) and is a reliable indicator of an extra-axial position(3).

Magnetic resonance spectroscopy (MRS) is used in cases where image findings are atypical. Meningiomas demonstrate increased choline and decreased creatine(3).

Diffusion weighted imaging has been used to distinguish between benign and atypical meningiomas. A recent prospective study of 24 patients showed a significantly lower preoperative ADC value in atypical meningiomas compared to benign meningiomas indicating restricted diffusion within the atypical group(22). If this finding is confirmed in larger studies, DWI may provide a reliable non-invasive method of differentiation between benign and atypical meningiomas.

On FDG-PET, meningiomas are universally avid. FDG-PET has also shown promise as a method of differentiating grades of meningioma, with high grade meningiomas showing a significantly higher uptake than low grade meningiomas(23).

*Perineural spread*

Imaging of perineural spread is more sensitive with MRI than CT(24). The first feature of perineural spread visible on imaging is caused by the breakdown of the blood-brain barrier, which results in increased permeability of the endoneurial capillaries. This process is demonstrated most conspicuously on post-contrast T1 fat suppressed sequences, seen as increased enhancement of the affected nerve. When the tumour cells proliferate further, the nerve's diameter increases. This process results in effacement of perineural fat by hypointense tumour, seen best on T1 non fat suppressed sequences. Finally, the nerve becomes compressed and infiltrated by tumour resulting in denervation muscle atrophy of the associated muscle groups. In the acute and sub acute phases, this process results in T2 hyperintensity and mild T1 post-contrast enhancement in the muscles. In the chronic phase, this process causes progressive fatty muscle atrophy on T1 and fast spin echo T2 sequences(16,25). CT can demonstrate the widening and destruction of the neural foramina seen in perineural tumour spread. CT can also demonstrate obliteration of the perineural fat at the foraminal openings or pterygopalatine fossa, though less conspicuously than non fat suppressed T1 MRI(16,26).

*Treatment*

Surgery is the primary means of treatment, allowing for definitive diagnosis, reduction in mass effect and the chance of a complete cure. The aim of surgery is to perform a complete resection of tumour, dura and abnormal surrounding bone. In skull base lesions, involvement of major cranial nerves and vessels often precludes complete resection. For these cases, a balance is struck between the completeness of resection and the morbidity associated with resection of the structures involved.

Preoperative embolisation is used to decrease intraoperative blood loss and reduce tumour volume. Major risks include embolisation outside the tumour field, carotid dissection, and an increased risk of acute haemorrhage due to tumour necrosis. As a result, neurosurgical consideration of preoperative embolisation and the choice of material used varies widely(4).

Adjuvant radiotherapy use depends primarily on the completeness of surgical resection. Following subtotal resection, adjuvant chemotherapy is widely deemed beneficial(27). Following gross total excision, the literature is conflicting, with multiple retrospective studies arriving at opposing conclusions when balancing the risks and benefits of adjuvant radiotherapy(28–31).

Clinical trials of antineoplastic medical therapies for the adjuvant treatment of atypical meningioma have shown promising results though no agents are clinically available at present(32).

*Prognosis*

Atypical meningiomas are more aggressive than benign meningiomas, with higher rates of recurrence (29%) and higher risk of transformation to malignant meningioma(33). Perineural tumour spread often precludes complete resection

and can cause irreversible neurological impairment. An early imaging diagnosis of these conditions would seem likely to result in a significant reduction in morbidity and mortality.

*Differential Diagnosis*

The appearance of a skull base tumour with perineural tumour spread can be caused by ascending extracranial tumours, descending intracranial tumours or tumours arising from the cranial nerves themselves.

*Ascending perineural spread*

Nasopharyngeal squamous cell carcinoma (SCC) is the most common cause of ascending perineural spread, occurring in 5-14% of cases(34). On T1 MRI, SCC is hypo- to isointense and commonly causes adjacent bone destruction. Post contrast, SCC exhibits mild, homogeneous enhancement. On T2 sequences, SCC is classically iso- to hyperintense and frequently causes markedly hyperintense obstructed middle ear secretions. CT commonly shows large necrotic lymph nodes and adjacent bone destruction. Fluorodeoxyglucose positron emission tomography (FDG-PET) examination shows marked avidity of the tumour and involved lymph nodes(35).

Adenoid cystic carcinoma of the salivary glands (ACC) is far less common than SCC but has a great propensity for perineural spread, which occurs in up to 60% of cases(36). On MRI, ACC is usually isointense on T1, iso- to hyperintense on T2 and exhibits moderate post contrast enhancement. CT demonstrates an infiltrative mass commonly causing erosion of the bones of the skull base, hard palate, maxilla and mandible. ACC is usually hypermetabolic on FDG-PET. Associated lymphadenopathy is an uncommon feature(37).

Non-Hodgkin lymphoma (NHL) is seen as a large mass on cross-sectional imaging. NHL is usually isointense on T1 MRI and exhibits moderate, homogeneous post contrast enhancement. The appearance of NHL on T2 sequences depends on the tumour cellularity, though it is classically isointense. CT shows non-necrotic bulky nodal disease in approximately 50% of cases, and frequently demonstrates deep invasion of the surrounding bones of the skull base. NHL is avid on FDG-PET(38).

*Nerve based tumours*

Trigeminal schwannomas classically arise from the mandibular branch of the trigeminal nerve. They are well-defined tumours, which extend intra- and extracranially along the path of least resistance. On MRI, Schwannomas are iso- to hypointense on T1 sequences and iso- to hyperintense on T2. Post-contrast, Trigeminal schwannomas can enhance homogeneously or heterogeneously, with interspersed non-enhancing intramural cysts considered characteristic. On CT, schwannomas classically cause smooth enlargement of the foramen ovale without bone erosion. Trigeminal schwannomas are avid on FDG-PET(39).

Solitary neurofibromas of the head and neck are rare and not usually associated with neurofibromatosis type 1(40). Neurofibromas are well-defined tumours that most commonly arise from the ophthalmic and maxillary branches of the trigeminal nerve. On MRI, neurofibromas are classically

hypointense on T1 sequences, hyperintense on T2 sequences and exhibit homogeneous post contrast enhancement. In some cases, they may possess a hypointense centre that enhances post contrast relative to the periphery (the “target sign”) or contain multiple small hypointense foci that represent fascicular bundles (the “fascicular sign”). Neurofibromas are classically hypoattenuating on CT (5-25 Hounsfield units) and cause smooth enlargement of the surrounding neural foramen. Solitary neurofibromas are FDG-PET avid(41).

#### TEACHING POINT

Perineural spread of a skull base tumour has a wide differential diagnosis. Skull base tumours are often difficult to access for biopsy, rendering radiological diagnosis of paramount importance. Though atypical meningioma is a rare cause of perineural spread, the high overall incidence of meningioma warrants its consideration in the differential diagnosis. When considered, the distinct imaging characteristics of meningioma such as a dural tail, internal calcification and hyperostosis of the adjacent bone differentiate it from other possible diagnoses.

#### REFERENCES

- Louis DN, Ohgaki H, Wiestler OD, Cavenee WK, Burger PC, Jouvet A, et al. The 2007 WHO classification of tumours of the central nervous system. *Acta Neuropathologica*. 2007. p. 97–109. PMID: 17618441
- Whittle IR, Smith C, Navoo P, Collie D. Meningiomas. *Lancet*. 2004 May 8;363(9420):1535–43. PMID: 15135603
- Watts J, Box G, Galvin A, Brotchie P, Trost N, Sutherland T. Magnetic resonance imaging of meningiomas: A pictorial review. *Insights into Imaging*. 2014. p. 113–22. PMID: 24399610
- Modha A, Gutin PH. Diagnosis and treatment of atypical and anaplastic meningiomas: A review. *Neurosurgery*. 2005. p. 538–49. PMID: 16145534
- Louis DN, Ohgaki H, Wiestler OD, Cavenee WK, Burger PC, Jouvet A, et al. The 2007 WHO classification of tumours of the central nervous system. *Acta Neuropathol*. 2007 Aug;114(2):97–109. PMID: 17618441
- Mahmood A, Caccamo D V., Tomecek FJ, Malik GM. Atypical and malignant meningiomas: a clinicopathological review. *Neurosurgery*. 1993 Dec;33(6):955–63. PMID: 8134008
- Nemzek WR, Hecht S, Gandour-Edwards R, Donald P, McKennan K. Perineural spread of head and neck tumors: How accurate is MR imaging? *American Journal of Neuroradiology*. 1998. p. 701–6. PMID: 9576658

- Barakos JA, Dillon WP. Lesions of the foramen ovale: CT-guided fine-needle aspiration. *Radiology*. 1992. p. 573–5. PMID: 1732985
- Wei FY, Wu CT, Lin KL, Wong AMC, Wong HF, Ng SH. Childhood atypical meningioma with perineural spread: MR findings. *Pediatr Radiol*. 2005;35:895–8. PMID: 15886983
- Weber RG, Boström J, Wolter M, Baudis M, Collins VP, Reifenberger G, et al. Analysis of genomic alterations in benign, atypical, and anaplastic meningiomas: toward a genetic model of meningioma progression. *Proc Natl Acad Sci U S A*. 1997;94:14719–24. PMID: 9405679
- Marosi C, Hassler M, Roessler K, Reni M, Sant M, Mazza E, et al. Meningioma. *Crit Rev Oncol Hematol*. 2008 Aug;67(2):153–71. PMID: 18342535
- Finn J, Mount L. Meningiomas of the tuberculum sellae and planum sphenoidale. A review of 83 cases. *Arch Ophthalmol*. 1974;92:23–7. PMID: 4835973
- Symon L, Jakubowski J. Clinical features, technical problems, and results of treatment of anterior parasellar meningiomas. *Acta Neurochir Suppl*. 1979;28:367–70. PMID: 290208
- Solero CL, Giombini S MG. Suprasellar and olfactory meningiomas. Report on a series of 153 personal cases. *Acta Neurochir*. 67(3-4):181–94. PMID: 6846075
- Maroldi R, Farina D, Borghesi A, Marconi A, Gatti E. Perineural tumor spread. *Neuroimaging Clin N Am*. 2008 May;18(2):413–29, xi. PMID: 18466839
- Ong CK, Chong VF-H. Imaging of perineural spread in head and neck tumours. *Cancer Imaging*. 2010 Jan;10 Spec no(October):S92–8. PMID: 20880778
- Mendenhall WM, Amdur RJ, Hinerman RW, Werning JW, Malyapa RS, Villaret DB, et al. Skin cancer of the head and neck with perineural invasion. *Am J Clin Oncol*. 2007;30:93–6. PMID: 17278901
- Warden KF, Parmar H, Trobe JD. Perineural spread of cancer along the three trigeminal divisions. *J Neuroophthalmol*. 2009 Dec;29(4):300–7. PMID: 19952904
- Catalano PJ, Sen C, Biller HF. Cranial neuropathy secondary to perineural spread of cutaneous malignancies. *Am J Otol*. 1995;16:772–7. PMID: 8572140
- Boerman RH, Maassen EM, Joosten J, Kaanders HA, Marres HA, van Overbeeke J, et al. Trigeminal neuropathy secondary to perineural invasion of head and neck carcinomas. *Neurology*. 1999;53:213–6. PMID: 10408563
- Rockhill J, Mrugala M, Chamberlain MC. Intracranial meningiomas: an overview of diagnosis and treatment. *Neurosurg Focus*. 2007;23:E1. PMID: 17961033

22. Toh CH, Castillo M, Wong AMC, Wei KC, Wong HF, Ng SH, et al. Differentiation between classic and atypical meningiomas with use of diffusion tensor imaging. *Am J Neuroradiol*. 2008;29:1630–5. PMID: 18583409
23. Lee JW, Kang KW, Park S-H, Lee SM, Paeng JC, Chung J-K, et al. 18F-FDG PET in the assessment of tumor grade and prediction of tumor recurrence in intracranial meningioma. *Eur J Nucl Med Mol Imaging*. 2009;36(10):1574–82. PMID: 19377904
24. Ginsberg LE. MR imaging of perineural tumor spread. *Neuroimaging Clinics of North America*. 2004. p. 663–77. PMID: 12530232
25. Fischbein NJ, Kaplan MJ, Jackler RK, Dillon WP. MR imaging in two cases of subacute denervation change in the muscles of facial expression. *Am J Neuroradiol*. 2001;22:880–4. PMID: 11337333
26. Caldemeyer KS, Mathews VP, Righi PD, Smith RR. Imaging features and clinical significance of perineural spread or extension of head and neck tumors. *Radiographics*. 1998;18:97–110. PMID: 9460111
27. Jenkinson M, Weber D, Haylock B, Mallucci C, Zakaria R, Javadpour M. Atypical meningioma: current management dilemmas and prospective clinical trials. *J Neurooncol*. Springer US; 2015;121(1):1–7. PMID: 25258253
28. Mair R, Morris K, Scott I, Carroll TA. Radiotherapy for atypical meningiomas. *Journal of Neurosurgery*. 2011. p. 811–9. PMID: 21699480
29. Komotar RJ, Iorgulescu JB, Raper DMS, Holland EC, Beal K, Bilsky MH, et al. The role of radiotherapy following gross-total resection of atypical meningiomas. *Journal of Neurosurgery*. 2012. p. 679–86. PMID: 22920955
30. Jo K, Park HJ, Nam DH, Lee J Il, Kong DS, Park K, et al. Treatment of atypical meningioma. *J Clin Neurosci*. 2010;17(11):1362–6. PMID: 20800497
31. Park HJ, Kang HC, Kim IH, Park SH, Kim DG, Park CK, et al. The role of adjuvant radiotherapy in atypical meningioma. *J Neurooncol*. 2013;115(2):241–7. PMID: 23949108
32. Yamaguchi S, Terasaka S, Kobayashi H, Asaoka K, Motegi H, Nishihara H, et al. Prognostic factors for survival in patients with high-grade meningioma and recurrence-risk stratification for application of radiotherapy. *PLoS One*. 2014 Jan;9(5):e97108. PMID: 24820480
33. Aghi MK, Carter BS, Cosgrove GR, Ojemann RG, Amin-Hanjani S, Martuza RL, et al. Long-term recurrence rates of atypical meningiomas after gross total resection with or without postoperative adjuvant radiation. *Neurosurgery*. 2009;64:56–60. PMID: 19145156
34. Fowler BZ, Crocker IR, Johnstone PAS. Perineural spread of cutaneous malignancy to the brain: A review of the literature and five patients treated with stereotactic radiotherapy. *Cancer*. 2005. p. 2143–53. PMID: 15816051
35. Goh J, Lim K. Imaging of nasopharyngeal carcinoma. *Annals of the Academy of Medicine Singapore*. 2009. p. 809–16. PMID: 19816641
36. Yousem DM, Gad K, Tufano RP. Resectability issues with head and neck cancer. *American Journal of Neuroradiology*. 2006. p. 2024–35. PMID: 17110661
37. Lee YYP, Wong KT, King AD, Ahuja AT. Imaging of salivary gland tumours. *Eur J Radiol*. 2008;66(3):419–36. PMID: 18337041
38. Aiken AH, Glastonbury C. Imaging Hodgkin and Non-Hodgkin Lymphoma in the Head and Neck. *Radiologic Clinics of North America*. 2008. p. 363–78. PMID: 18619385
39. Beaulieu S, Rubin B, Djang D, Conrad E, Turcotte E, Eary JF. Positron Emission Tomography of Schwannomas: Emphasizing Its Potential in Preoperative Planning. *Am J Roentgenol*. 2004;182:971–4. PMID: 15039173
40. Kami YN, Chikui T, Okamura K, Kubota Y, Oobu K, Yabuuchi H, et al. Imaging findings of neurogenic tumours in the head and neck region. *Dentomaxillofac Radiol*. 2012;41(1):18–23. PMID: 22074867
41. Lin J, Martel W. Cross-Sectional Imaging of Peripheral Nerve Sheath Tumors. 2012;(January):75–82. PMID: 11133542

## FIGURES

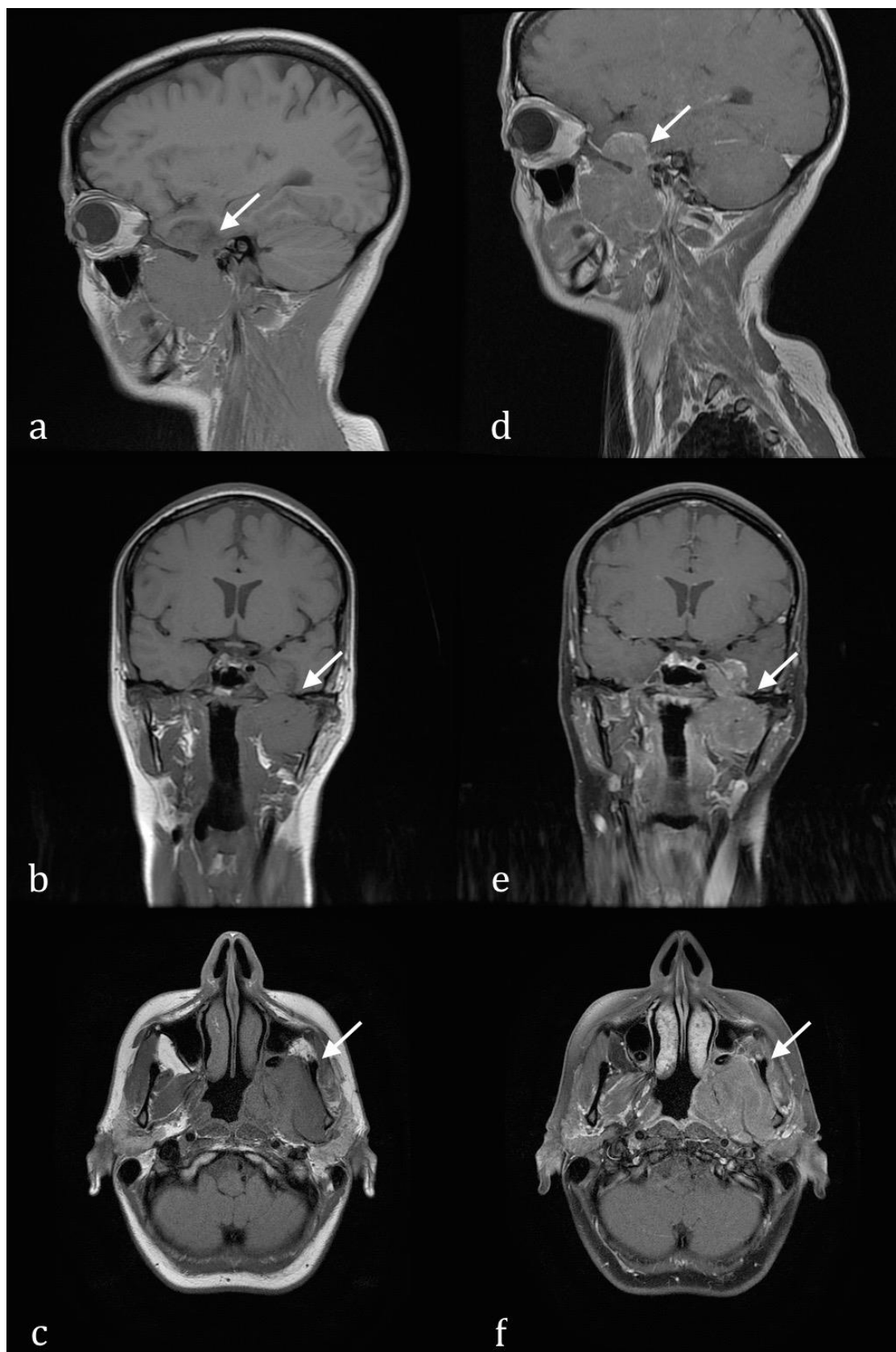


**Figure 1:** 46-year-old female with an atypical skull base meningioma. FINDINGS: Pre contrast (a-c) and post contrast fat-saturated (d-f) T1 sagittal, coronal and axial sections demonstrating maximal tumour dimensions, isointense tumour signal pre contrast and homogeneous tumour enhancement post contrast. TECHNIQUE: GE Medical Systems Discovery MR450 1.5 Tesla, (a-c) Pre contrast T1 Fast Spin Echo (FSE): TR 545ms, TE 16.64ms. (d-f) Post contrast fat saturated FSE: TR 627ms, TW16.64. Gadolinium intravenous contrast.

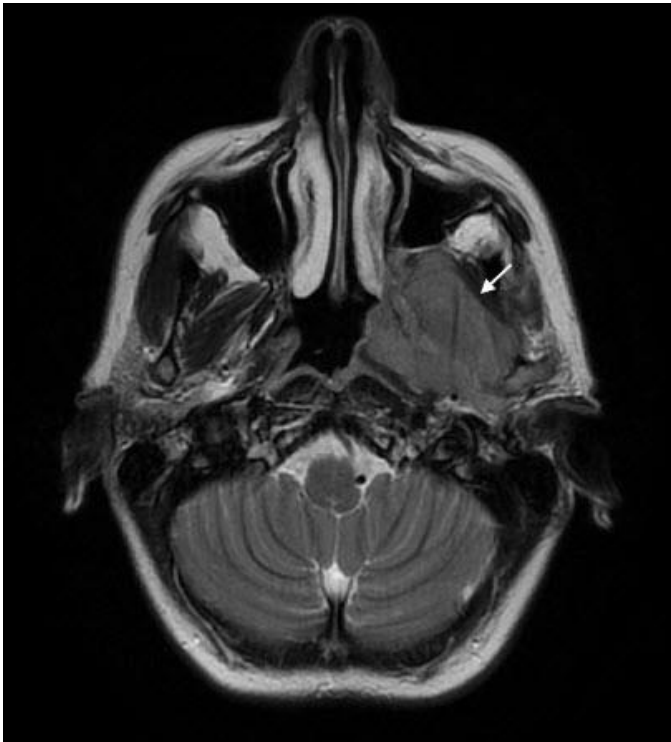


**Figure 2:** 46-year-old female with an atypical skull base meningioma. FINDINGS: T2 axial section demonstrating iso- to hyperintense tumour signal. TECHNIQUE: GE Medical Systems Discovery MR450 1.5 Tesla, T2 Fast Spin echo, TR 6790ms, TE 98.98ms.

**Figure 4:** 46-year-old female with an atypical skull base meningioma. FINDINGS: T2 axial sections demonstrating extension of tumour into the nasopharynx (white arrow) resulting in obstruction of the left Eustachian tube and fluid opacification of the left mastoid air cells (red arrows). TECHNIQUE: GE Medical Systems Discovery MR450 1.5 Tesla. T2 FSE: TR 6790ms, TE 98.98ms.

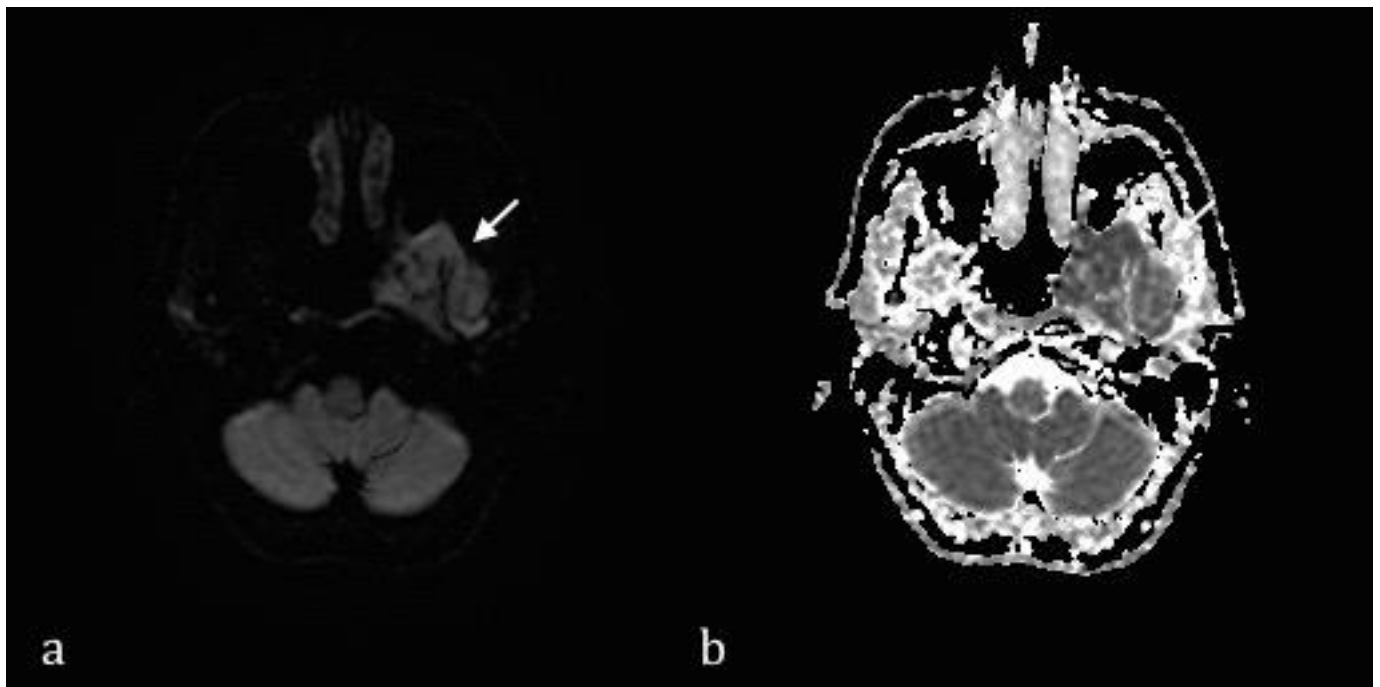


**Figure 3:** 46-year-old female with an atypical skull base meningioma. FINDINGS: Diffusion Weighted Imaging (b1000) and Apparent Diffusion Coefficient axial sections demonstrating restricted diffusion on DWI images (a) and a low ADC value (b). TECHNIQUE: GE Medical Systems Discovery MR450 1.5 Tesla, Diffusion Weighted Imaging and Apparent Diffusion Coefficient, TR 8000ms, TE 82.6ms.

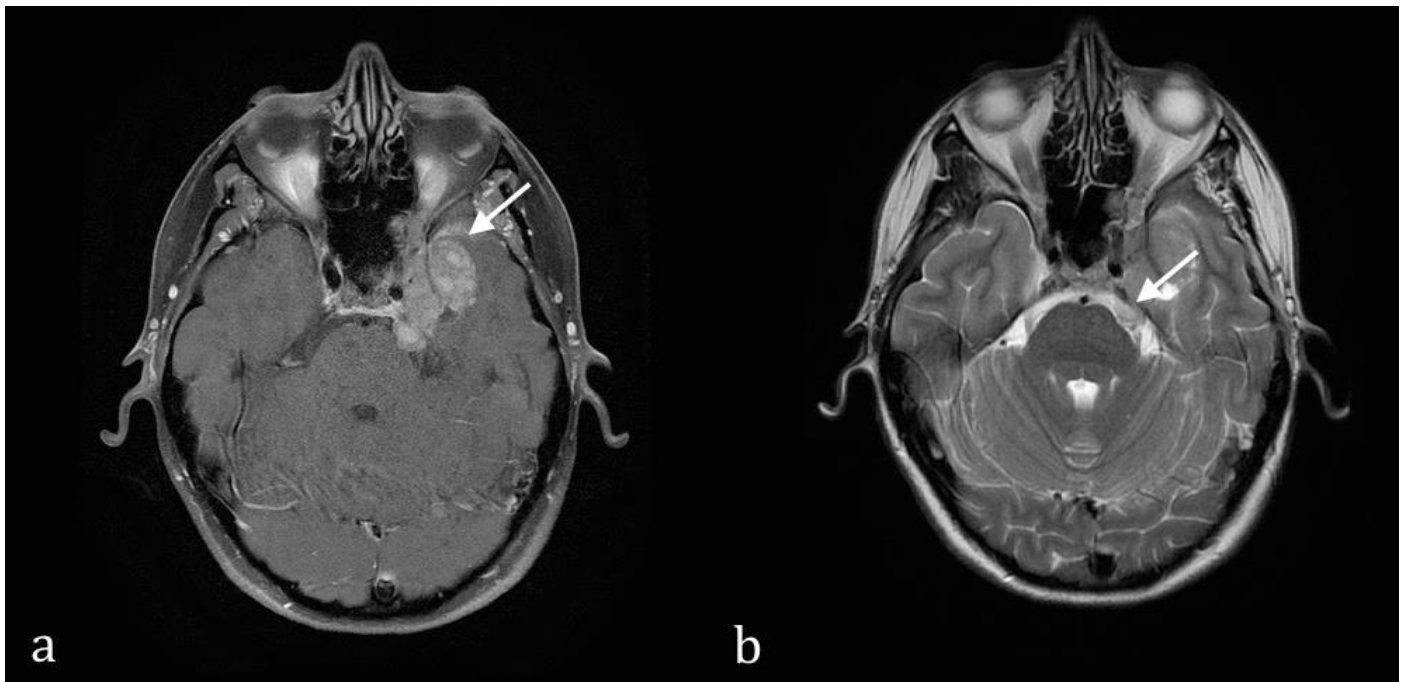


**Figure 5:** 46-year-old female with an atypical skull base meningioma. FINDINGS: Post contrast T1 fat-saturated (a) and T2 (b) axial sections showing (a) tumour within the cavernous sinus and Meckel's cave invading into the sphenoid sinus anteriorly and (b) tumour in the prepontine cistern, inseparable on imaging from the proximal trigeminal nerve. TECHNIQUE: GE Medical Systems Discovery MR450 1.5 Tesla. (a) Post contrast T1 fat saturated FSE, TR 627ms, TE16.64. Gadolinium intravenous contrast. (b) T2 FSE, TR6790, TE 98.98.

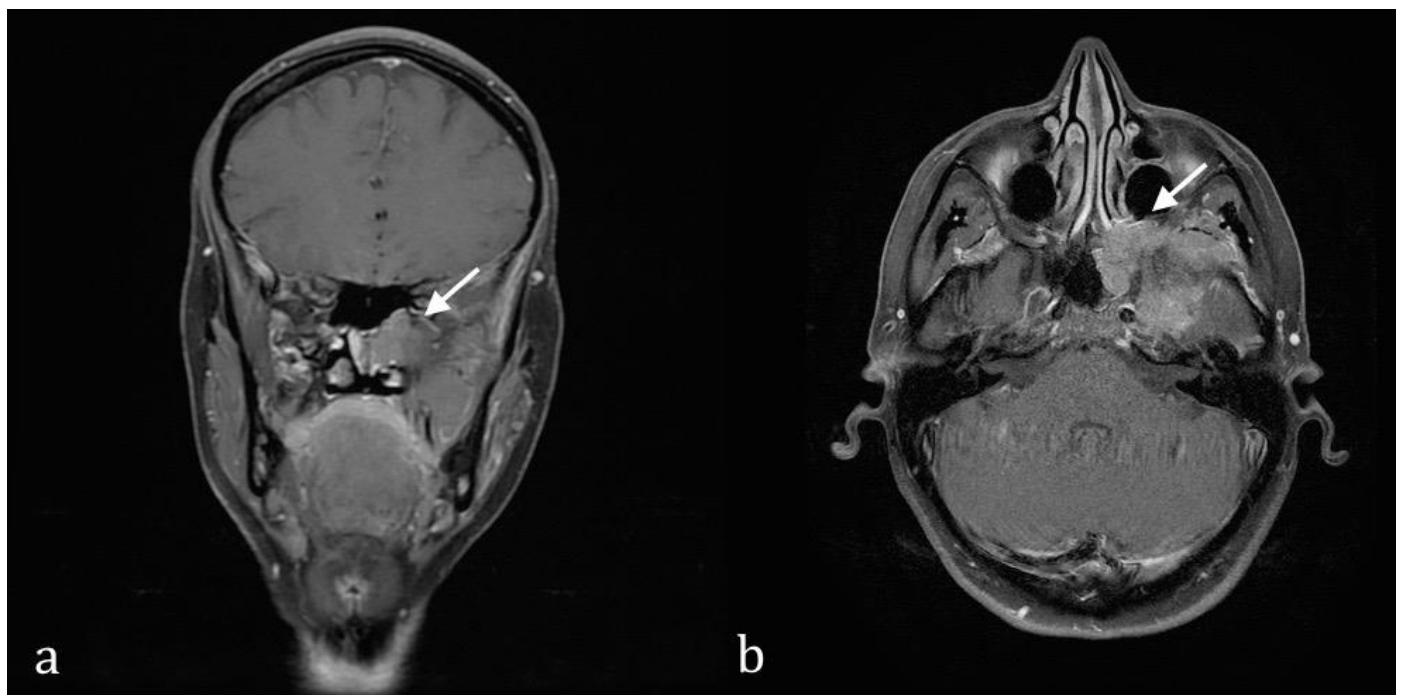


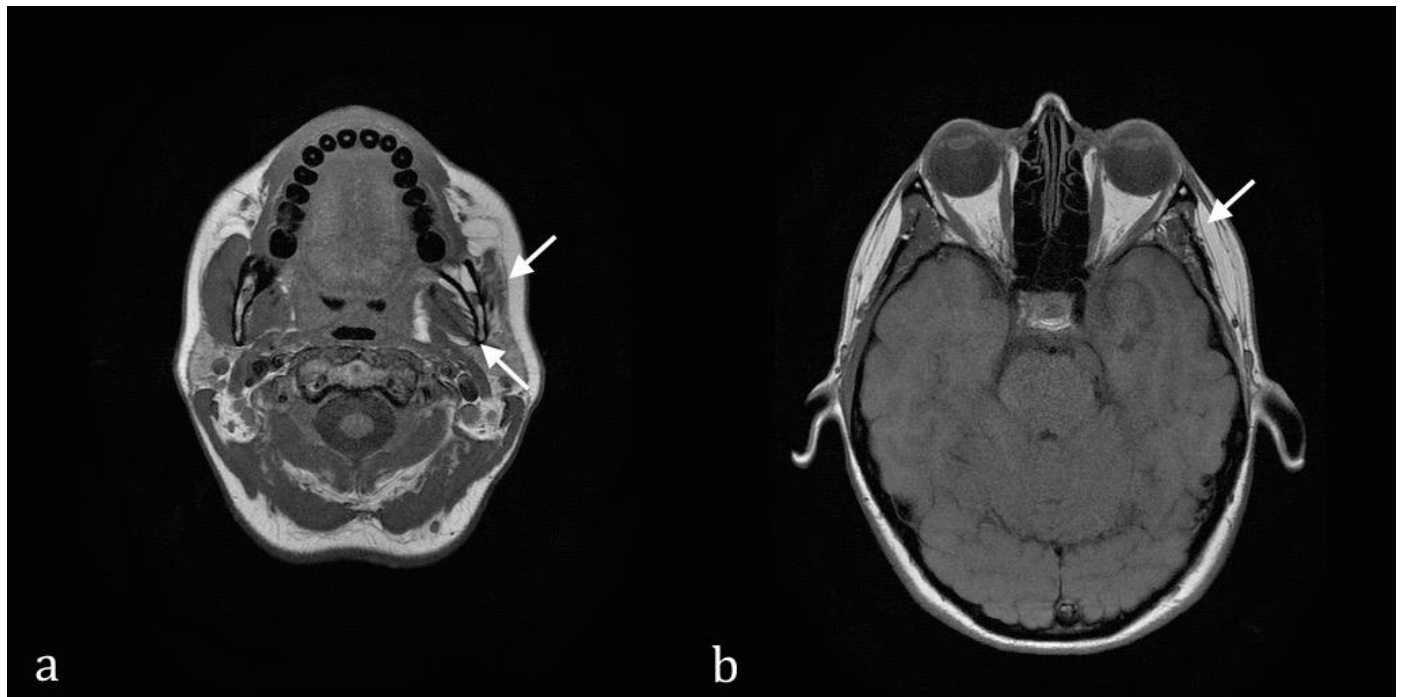
**Figure 6:** 46-year-old female with an atypical skull base meningioma. FINDINGS: Post-contrast T1 fat saturated coronal and axial sections demonstrating tumour eroding through (a) the wall of the sphenoid sinus and (b) through the sphenopalatine foramen into the nasal cavity. TECHNIQUE: GE Medical Systems Discovery MR450 1.5 Tesla. Post contrast fat saturated FSE: TR 627 ms, TW16.64. Gadolinium intravenous contrast.





**Figure 7 (left):** 46-year-old female with an atypical skull base meningioma. FINDINGS: Axial CT section demonstrating widening of the sphenopalatine foramen and tumour extension into the nasopharynx. TECHNIQUE: Non contrast axial CT, 130 mAs, 120 kV, 1.5mm slice thickness.

**Figure 8 (bottom):** 46-year-old female with an atypical skull base meningioma. FINDINGS: Pre contrast T1 axial sections demonstrating denervation atrophy of the (a) pterygoid and masseter muscles and (b) temporalis muscle on the left side due to long-standing perineural spread. TECHNIQUE: GE Medical Systems Discovery MR450 1.5 Tesla. Pre contrast T1 FSE, TR 545ms, TE 16.64ms.



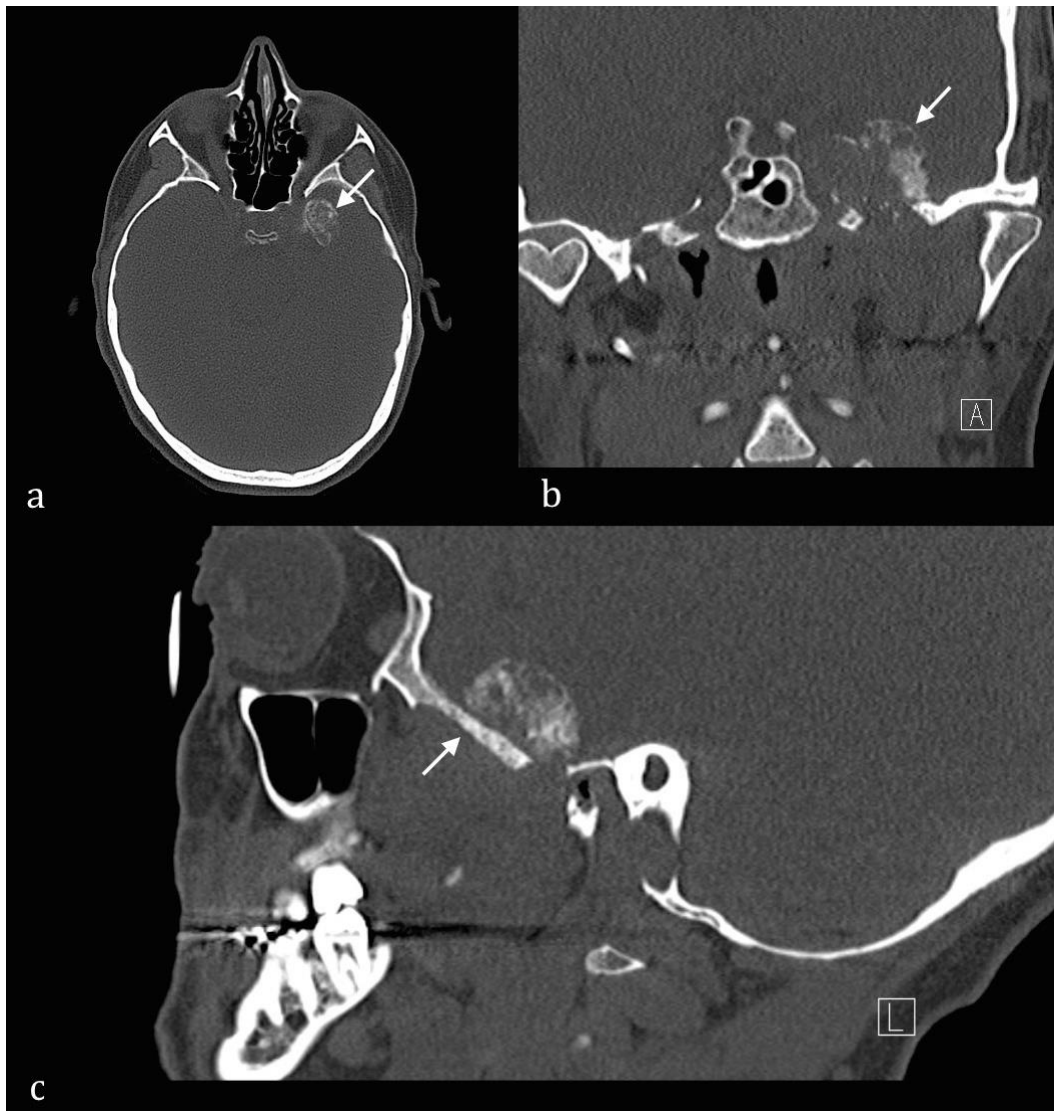


**Figure 9:** 46-year-old female with an atypical skull base meningioma. FINDINGS: Axial, coronal and sagittal CT sections demonstrating internal calcification of the intracranial portion of the mass and hyperostosis and erosion of the greater wing of the sphenoid. TECHNIQUE: Non contrast axial CT with coronal and sagittal reconstructions, 218mAs, 120 kV, 1.5mm slice thickness.



**Figure 10 (left):** 46-year-old female with an atypical skull base meningioma. FINDINGS: Axial CT of the skull base demonstrating tumour extending into the nasopharynx (white arrow) with associated erosion of the left pterygoid plate and posterior maxillary alveolus (red arrow). TECHNIQUE: Non-contrast axial CT, 218mAs, 120 kV, 1.5mm slice thickness.

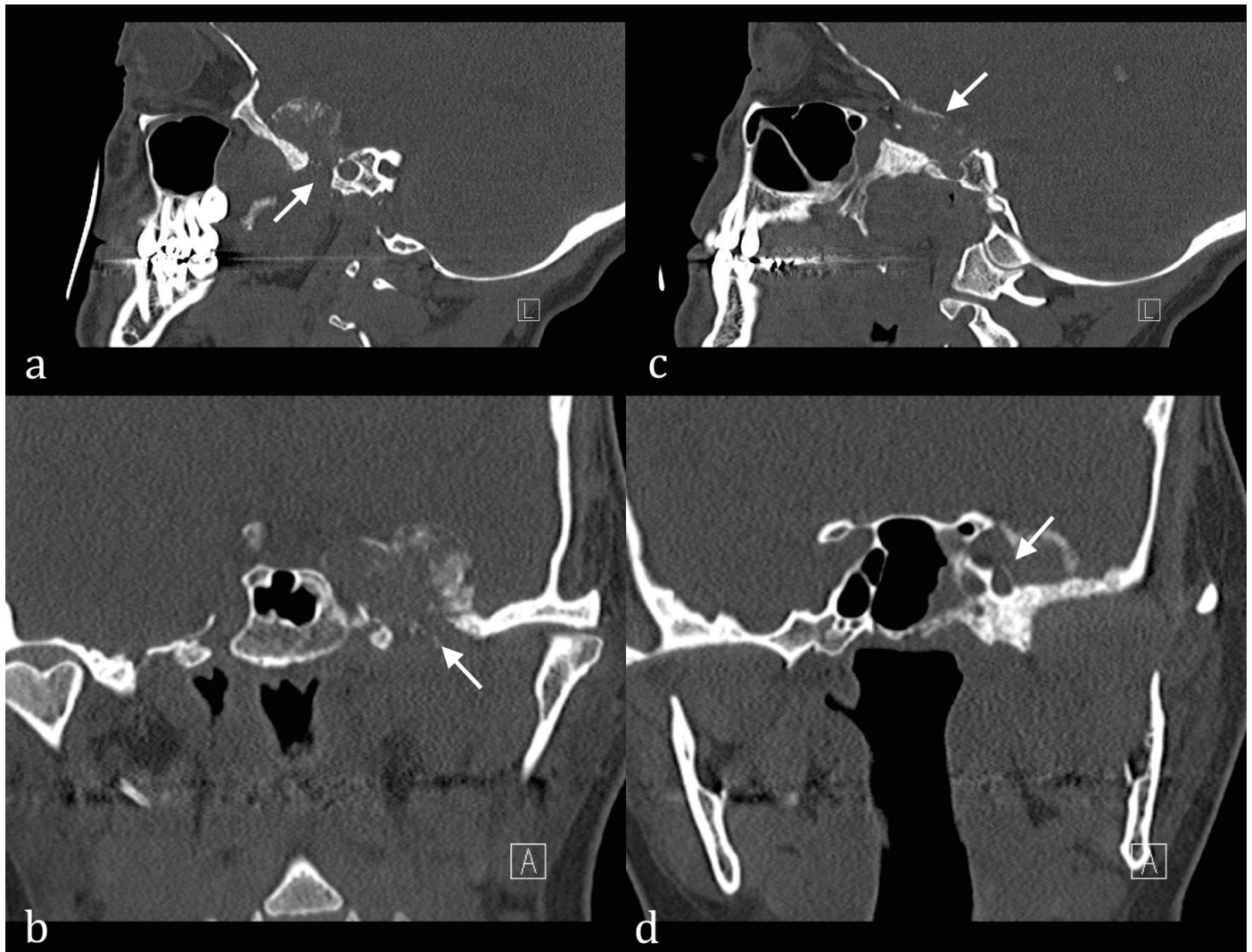


**Figure 11:** 46-year-old female with an atypical skull base meningioma. FINDINGS: Sagittal (a,c) and Coronal (b,d) CT sections demonstrating foramen ovale expansion(a,b) and foramen rotundum expansion (c,d) with hyperostosis of the surrounding sphenoid wing. TECHNIQUE: Non contrast axial CT, 218mAs, 120kV, 1.5mm slice thickness.

Journal of Radiology Case Reports

www.RadiologyCases.com



**Figure 12 (left):** 46-year-old female with an atypical skull base meningioma. FINDINGS: Axial CT section demonstrating mixed hyperostosis and erosion of the greater wing of the sphenoid. TECHNIQUE: Non-contrast axial CT, 218mAs, 120kV, 1.5mm slice thickness.

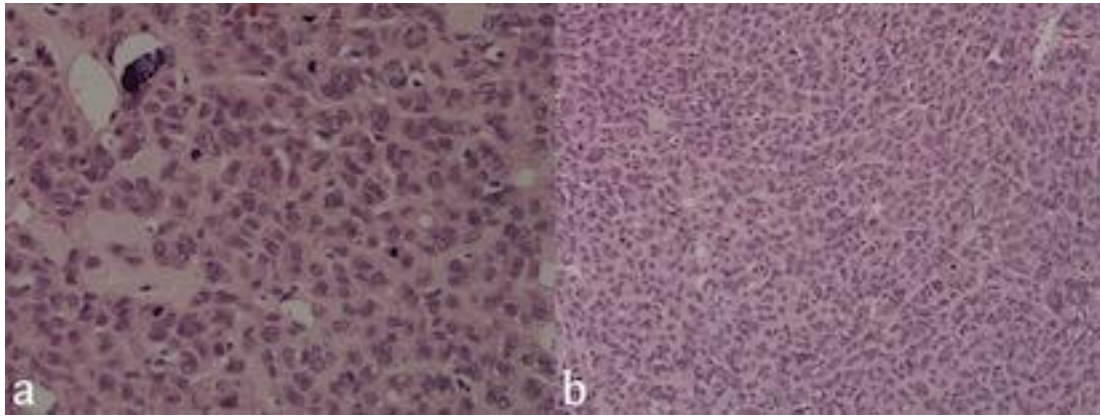


**Figure 13:** 46-year-old female with an atypical skull base meningioma. FINDINGS: Pathological sections showing (a) increased mitotic activity and prominent nucleoli at 40x magnification and (b) uninterrupted patternless, sheet-like growth at 20x magnification. These are key diagnostic features of atypical meningioma. TECHNIQUE: Hematoxylin-eosin stained core biopsy sections at (a) 40x and (b) 20x magnification.

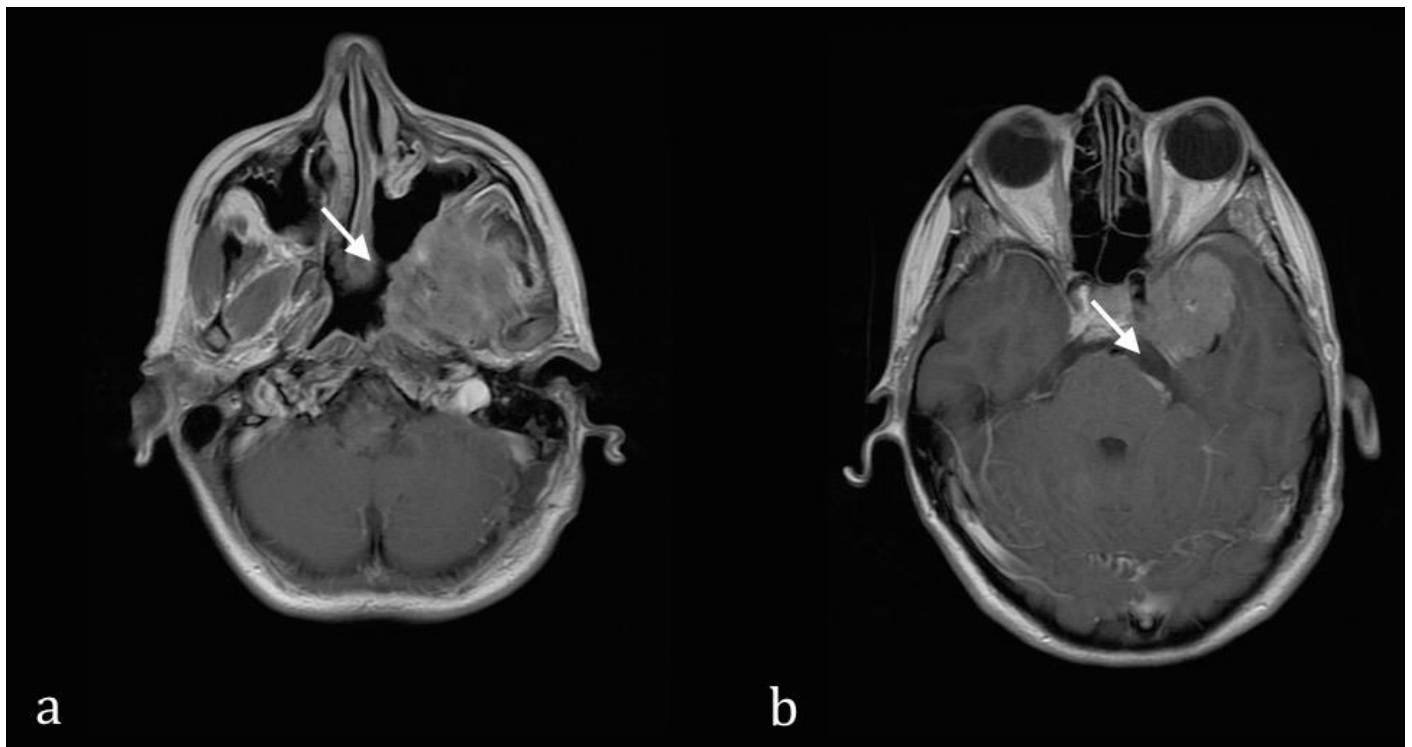


**Figure 14:** 46-year-old female with an atypical skull base meningioma. FINDINGS: Post contrast T1 axial sections showing the post-operative appearances of the tumour following (a) maxillotomy to debulk the extracranial portion of tumour and (b) a posterior fossa craniotomy to excise of the cerebellopontine angle tumour. TECHNIQUE: GE Medical Systems Discovery MR450 1.5 Tesla, Post contrast T1 FSE: TR 552ms, TE 10.41. Gadolinium intravenous contrast.

<b>Etiology</b>	<ul style="list-style-type: none"> <li>• Genetic mutation at chromosome 22q12 causes the loss of tumour suppressor protein</li> <li>• Loss of tumour suppressor protein “Schwannomin” causes an increased risk of developing benign meningiomas.</li> <li>• Further accumulation of chromosomal mutations leads to transformation to atypical and malignant meningioma.</li> </ul>
<b>Incidence</b>	<ul style="list-style-type: none"> <li>• 4.7-7.2% of all meningiomas.</li> <li>• Approximately 3 in 1,000,000.</li> </ul>
<b>Gender ratio (M:F)</b>	<ul style="list-style-type: none"> <li>• 1:0.9 (compared to 1:2.3 for benign meningiomas)</li> </ul>
<b>Ethnicity</b>	<ul style="list-style-type: none"> <li>• Benign meningiomas are common in African-Americans.</li> <li>• No ethnic predominance has been seen in small studies of atypical meningioma.</li> </ul>
<b>Age predilection</b>	<ul style="list-style-type: none"> <li>• Middle age, approximately 10 years earlier than benign meningioma.</li> </ul>
<b>Risk factors</b>	<ul style="list-style-type: none"> <li>• Neurofibromatosis Type 2</li> <li>• Previous ionising radiation exposure.</li> </ul>
<b>Treatment</b>	<ul style="list-style-type: none"> <li>• Surgery +/- adjuvant radiotherapy +/- preoperative embolisation</li> </ul>
<b>Prognosis</b>	<ul style="list-style-type: none"> <li>• 5-year survival: 86%, 10 year survival: 61%</li> <li>• 5-year recurrence free survival: 48%</li> <li>• Overall recurrence: 26%</li> <li>• Median time to recurrence: 3 years</li> </ul>
<b>MR imaging</b>	<ul style="list-style-type: none"> <li>• CSF cleft (80%); Dural tail (58%)</li> <li>• T1: iso- to hypointense</li> <li>• T2: iso- to hyperintense</li> <li>• +C: Homogeneously enhancing</li> <li>• MRS: High choline, Low creatine</li> <li>• DWI: Decreased ADC values</li> </ul>
<b>CT imaging</b>	<ul style="list-style-type: none"> <li>• Homogeneous hyperattenuation (72%)</li> <li>• Frequently tumoral calcification (18%)</li> <li>• Peritumoral vasogenic oedema (52%)</li> <li>• Hyperostosis of the adjacent bone (18%)</li> </ul>
<b>FDG-PET imaging</b>	<ul style="list-style-type: none"> <li>• FDG- avid</li> </ul>

**Table 1:** Summary table for atypical skull base meningioma.

	<b>MRI</b>	<b>CT</b>	<b>PET/CT</b>
<b>Atypical meningioma</b>	<ul style="list-style-type: none"> <li>• T1: Iso- to hypointense</li> <li>• T2: Iso- to hyperintensity.</li> <li>• T2: CSF cleft</li> <li>• T1+C: Homogeneous enhancement</li> <li>• T1+C: Enhancing dural tail</li> <li>• MRS: High choline, low creatinine</li> <li>• DWI: Decreased ADC values</li> </ul>	<ul style="list-style-type: none"> <li>• Tumoral calcification (20%)</li> <li>• Expansion +/- erosion of neural foramina</li> </ul>	<ul style="list-style-type: none"> <li>• FDG avid</li> </ul>
<b>Squamous Cell Carcinoma</b>	<ul style="list-style-type: none"> <li>• T1: Hypo- or isointense</li> <li>• T2: Iso- to hyperintense</li> <li>• T2: Hyperintense obstructed middle ear secretions</li> <li>• T1+C: Mild, homogeneous enhancement</li> </ul>	<ul style="list-style-type: none"> <li>• Large necrotic lymph nodes</li> <li>• Bony destruction</li> </ul>	<ul style="list-style-type: none"> <li>• FDG avid tumour, lymph nodes and metastases</li> </ul>
<b>Adenoid cystic carcinoma</b>	<ul style="list-style-type: none"> <li>• T1: Isointense</li> <li>• T2: Iso- to hyperintense</li> <li>• T1+C: Moderate, homogeneous enhancement</li> </ul>	<ul style="list-style-type: none"> <li>• Erosion of the mandible or maxilla.</li> <li>• Enlarged lymph nodes not usually a feature</li> </ul>	<ul style="list-style-type: none"> <li>• FDG avid</li> </ul>
<b>Non-Hodgkin Lymphoma</b>	<ul style="list-style-type: none"> <li>• T1: Isointense</li> <li>• T2: Variable depending on tumour cellularity usually isointense</li> <li>• T1+C: Moderate, homogeneous enhancement</li> </ul>	<ul style="list-style-type: none"> <li>• Hyperdense</li> <li>• Non-necrotic bulky lymph nodes (50%)</li> <li>• Deep erosion of the surrounding bone</li> </ul>	<ul style="list-style-type: none"> <li>• FDG avid</li> </ul>
<b>Schwannoma of CNV3</b>	<ul style="list-style-type: none"> <li>• T1: Iso- to hypointense</li> <li>• T2: Iso- to hyperintense</li> <li>• T1+C: Variable enhancement pattern</li> <li>• T1+C: Intratumoral cysts are characteristic</li> </ul>	<ul style="list-style-type: none"> <li>• Smooth enlargement of foramen ovale without erosion.</li> </ul>	<ul style="list-style-type: none"> <li>• FDG avid</li> </ul>
<b>Neurofibroma of CNV3</b>	<ul style="list-style-type: none"> <li>• T1: Hypointense</li> <li>• T1: "Target sign" - hypointense centre with hyperintense periphery</li> <li>• T1: "Fascicular sign" - multiple small hypointense foci</li> <li>• T2: Hyperintense</li> <li>• T1+C: Homogeneous enhancement</li> <li>• T1+C: "Target sign" - centre enhances relative to periphery</li> </ul>	<ul style="list-style-type: none"> <li>• Hypodense (5-25 HU)</li> <li>• Smooth enlargement of neural foramina</li> </ul>	<ul style="list-style-type: none"> <li>• FDG avid</li> </ul>

**Table 2:** Differential diagnosis table for atypical skull base meningioma with perineural spread.

#### ABBREVIATIONS

ACC – Adenoid cystic carcinoma  
 ADC – Apparent diffusion coefficient  
 CSF – Cerebrospinal fluid  
 CT – Computed tomography  
 DWI – Diffusion weighted imaging  
 FDG-PET - Fluorodeoxyglucose positron emission tomography  
 MRI – Magnetic resonance imaging  
 MRS – Magnetic resonance spectroscopy  
 NF2 – Neurofibromatosis type 2  
 NHL – Non- Hodgkin lymphoma  
 SCC – Squamous cell carcinoma  
 WHO – World health organisation

#### KEYWORDS

Atypical meningioma; perineural spread; skull base tumour; skull base mass

#### Online access

This publication is online available at:  
[www.radiologycases.com/index.php/radiologycases/article/view/2648](http://www.radiologycases.com/index.php/radiologycases/article/view/2648)

#### Peer discussion

Discuss this manuscript in our protected discussion forum at:  
[www.radiopolis.com/forums/JRCR](http://www.radiopolis.com/forums/JRCR)

#### Interactivity

This publication is available as an interactive article with scroll, window/level, magnify and more features.  
 Available online at [www.RadiologyCases.com](http://www.RadiologyCases.com)

Published by EduRad



[www.EduRad.org](http://www.EduRad.org)